Received: 10 May 2021 | Accepted: 29 June 2021

DOI: 10.1111/1759-7714.14082

ORIGINAL ARTICLE

WILEY

Mathematical prediction model of computed tomography signs is superior to intraoperative frozen section in the diagnosis of ground-glass nodular invasive adenocarcinoma of the lung

Jizheng Tang | Yong Cui | Bowen Li | Xingxing Xue | Feng Tian

Department of Thoracic Surgery, Beijing Friendship Hospital of Capital Medical University, Beijing, China

Correspondence
Feng Tian, Department of Thoracic Surgery, Beijing Friendship Hospital of Capital Medical University, Beijing 100050, China.
Email: tianfeng62@aliyun.com

Abstract

Background: At present, lobectomy is still the standard treatment for lung cancer. Judging whether a lesion is invasive adenocarcinoma (IA) has important guiding significance for determining the scope of surgical resection. The commonly used methods are intraoperative frozen sections and computed tomography (CT) signs. There is still controversy about the accuracy of both in judging the invasiveness of ground-glass nodules (GGNs).

Methods: The clinical data of patients with GGNs who underwent surgery were collected. According to the results of univariate analysis, the variables with statistical differences were selected and included in logistic regression multivariate analysis. The predictive variables were determined and the receiver operating characteristic (ROC) curve was drawn in order to achieve the area under the curve (AUC) value.

Results: According to the results of logistic regression analysis, the longest diameter and maximum CT value of nodules were independent risk factors for IA. The mathematical prediction model of CT signs was determined, and the ROC curves of CT signs and intraoperative frozen sections (FS) were drawn, respectively. The AUC values under the curves were calculated to be 0.873 and 0.807, respectively. The mathematical prediction model of intraoperative frozen section combined with CT signs was established. A ROC curve was drawn and the AUC was calculated to be 0.925.

Conclusions: The diagnostic accuracy of CT signs in judging whether nonbenign GGNs were IA was higher than that of intraoperative FS. Combined with CT signs and intraoperative FS to establish a mathematical prediction model, the diagnostic accuracy of judging whether nonbenign GGNs are IA is significantly improved.

KEYWORDS
ground glass nodule, mathematical prediction model, pulmonary invasive adenocarcinoma, receiver operating characteristic (ROC) curve

INTRODUCTION

Lung cancer has become the malignant tumor with the highest mortality rate in the world.[1,2] Early detection, together with early treatment can effectively reduce lung cancer mortality,[2] and therefore lung cancer screening is particularly important in clinical practice. According to the results of the National Lung Screening Trial (NLST), low-dose computed tomography (LDCT) is an effective screening method for high-risk groups.[3] With the popularity of lung computed tomography (CT) screening, the incidence of pulmonary nodules has significantly increased, and "speckled" lesions in the lung area are defined as pulmonary nodules. According to the content of solid components, pulmonary nodules can be divided into solid nodules and ground-glass nodules (GGNs). A GGN is defined as a slightly hyperdense shadow on CT,

Jizheng Tang and Yong Cui contributed equally to this work.

which does not mask the bronchial and vascular texture,[4,5] including pure ground-glass nodules (pGGNs) and mixed ground-glass nodules (mGGNs). In clinical practice, GGNs on CT are more challenging because of their potential malignancy and heterogeneity.[6]

According to the 2011 International Association for the Study of Lung Cancer (IASLC)/American Thoracic Society (ATS)/European Respiratory Society (ERS) standard classification of lung adenocarcinoma,[7] GGNs are often diagnosed as atypical adenomatoid hyperplasia (AAH), adenocarcinoma in situ (AIS), minimally invasive adenocarcinoma (MIA), and invasive adenocarcinoma (IA) in pathological diagnosis.[8] Although the radiological "GGN-type" lung adenocarcinoma has the histological and morphological characteristics of lung adenocarcinoma, it is a relatively inert subtype and its management and treatment should be different than that of "solid nodular" lung adenocarcinoma. Intraoperative frozen sections (FS) are most often used to evaluate uncertain lung lesions and guide surgical treatment,[9] but there is still room for improvement in the accuracy of intraoperative FS, especially for the differentiation of AAH, AIS, MIA and IA. In recent years, with the rapid development of CT, the evaluation of benign, malignant and invasive CT signs of pulmonary nodules has become very useful. The most common signs of nodules are nodule size, lobulation sign, spiculation sign, pleural traction, vascular convergence sign, air bronchial sign and so on.

FS and CT signs are of great significance in the management and surgical treatment of GGNs, but have their own limitations. The purpose of this study was to compare the accuracy of FS and CT signs mathematical prediction model in the diagnosis of GGN invasiveness, and to establish a mathematical prediction model combined with FS and CT signs.

METHODS

The clinical data of patients who underwent surgery in our hospital from June 1, 2018 to June 30, 2020 were collected continuously during this period. All patients underwent comprehensive examination before operation. Inclusion criteria were as follows: (i) chest CT imaging showed GGNs, (ii) the interval between chest CT scan and surgery was within one month, (iii) there was no preoperative radiotherapy and chemotherapy, and (iv) intraoperative frozen and paraffin-embedded tissue sections for pathological evaluation were available. Exclusion criteria were: (i) the quality of the CT image was poor, and (ii) clinical data was incomplete. According to the inclusion and exclusion criteria, a total of 272 patients were enrolled in the study, and CT images and pathological data (frozen and paraffin-embedded tissue sections) were collected. The study was approved by the Institutional Review Board of Beijing Friendship Hospital of Capital Medical University (No: 2020-P2-260-01).

The examination was performed with a GE Revolution 256 row spiral CT. The patient was asked to lay on their back with hands placed near their head. Images were collected from the entrance level of the chest to below the base of the lung. Scanning mode: the tube voltage was 120 kV, automatic tube current, pitch of 0.984:1, rotation time of 0.5 s, image thickness of 1.25 mm, and the interval between layers was 1.25 mm. The image was obtained by setting the mediastinal window (width 400 HU; level 40 HU) and lung window (width 1600 HU; level-700 HU). Two chest radiologists examined the CT data of all patients and were unaware of the pathological findings of the lesions. Differences in interpretation, if any, were resolved through negotiation. The following features of the lesions were evaluated on CT images: nodular type, nodular morphology, longest diameter of nodules, longest diameter of solid components, solid components of mediastinal window, vascular convergence sign, air bronchus sign, lobulation sign, spiculation sign, pleural traction, and maximum CT value (lung window).

According to the paraffin-embedded tissue section pathology, 272 patients were divided into two groups: the IA group and AAH/AIS/MIA groups. The clinical data of each group were statistically analyzed. Continuous variables are expressed as mean ± standard deviation (mean ± SD), while classified variables are expressed as absolute numbers. Independent sample *t*-test was used to compare the age, the longest diameter of nodules, the maximum CT value and the longest diameter of solid components among different groups. $\chi 2$ test was used to compare the sex, nodule type, nodule shape, solid composition of mediastinal window, vascular convergence sign, air bronchus sign, lobulation sign, spiculation sign, pleural traction and intraoperative frozen sections of patients in each group. Binary logistic regression analysis was used to screen independent risk factors for IA and to establish a mathematical predictive model. The receiver operating characteristic (ROC) curve was used to calculate the accuracy of the mathematical prediction model for the prediction of IA. All statistical analyses were performed using SPSS (IBM SPSS, Statistics for Windows, Version 22.0). All data statistics were conducted using a bilateral test, and statistical significance was set at $p < 0.05$.

RESULTS

According to the paraffin-embedded tissue section pathology, there were 166 cases in the AAH/AIS/MIA group (AAH 10 cases, AIS 69 cases, MIA 87 cases) and IA group (106 cases). Among the quantitative variables, there were significant differences in age ($p = 0.002$), longest diameter of nodules ($p < 0.001$), maximum CT value ($p = 0.008$) and longest diameter of solid components ($p < 0.001$) between the AAH/AIS/MIA and IA groups. Among the qualitative variables, there were significant differences in lobulation sign ($p < 0.001$), spiculation sign ($p < 0.001$), pleural traction ($p < 0.001$), intraoperative frozen section ($p < 0.001$), nodule type ($p < 0.001$), nodule shape ($p < 0.001$), mediastinal window solid component ($p < 0.001$) and air bronchus sign ($p < 0.001$) between the two groups. There was no significant difference in gender ($p = 0.275$) and vascular convergence sign ($p = 0.058$). Further details are given in Table 1 and Table 2.

TABLE 1 The quantitative variables and results of univariate analysis

Quantitative variables	AAH/AIS/MIA ($n = 166$) (mean ± SD, range)	IA ($n = 106$) (mean ± SD, range)	*p*-value
Age (year)	58.00 ± 11.12	62.12 ± 9.89	0.002
	(28–83)	(35–81)	
Longest diameter (cm)	1.18 ± 0.43	1.95 ± 0.78	<0.001
	(0.55–2.67)	(0.60–4.44)	
Maximum CT value (HU) of ROI	−304.81 ± 208.91	−56.08 ± 130.73	0.008
	(−749–60)	(−445–90)	
Longest diameter of solid components (cm)	0.30 ± 0.40	0.92 ± 0.63	<0.001
	(0–1.88)	(0–3.23)	

Abbreviations: AAH, atypical adenomatoid hyperplasia; AIS, adenocarcinoma in situ; CT, computed tomography; IA, invasive adenocarcinoma; MIA, minimally invasive adenocarcinoma; ROI, region of interest.

TABLE 2 The qualitative variables and the results of univariate analysis

Variables		AAH/AIS/MIA ($n = 166$)	IA ($n = 106$)	*p*-value
Gender	Male	49	38	0.275
	Female	117	68	
Lobulation	Yes	50	67	<0.001
	No	116	39	
Spiculation	Yes	57	71	<0.001
	No	109	35	
Pleural traction	Yes	44	62	<0.001
	No	122	44	
Type	pGGN	89	11	<0.001
	mGGN	77	95	
Shape	Quasicircular	85	14	<0.001
	Irregular	81	92	
Solid components of mediastinal window	Yes	40	80	<0.001
	No	126	26	
Vascular convergence	Yes	97	74	0.058
	No	69	32	
Air bronchial	Yes	15	37	<0.001
	No	151	69	
Intraoperative frozen section	AAH/AIS/MIAIA	163	39	<0.001
		3	67	

Abbreviations: AAH, atypical adenomatoid hyperplasia; AIS, adenocarcinoma in situ; IA, invasive adenocarcinoma; mGGN, mixed ground-glass nodule; MIA, minimally invasive adenocarcinoma; pGGN, pure ground-glass nodule.

According to the results of univariate analysis, two groups of mathematical prediction models were established. One group was not included in the FS, and the longest diameter, maximum CT value, pleural traction, nodular type, nodular shape, age, longest diameter of solid components, solid components of mediastinal window, lobulation sign, spiculation sign and air bronchus sign were included in the logistic regression analysis. The results showed that the longest diameter and maximum CT value of nodules were independent risk factors for IA, and the risk ratios were 4.426 (95% CI: 2.391–8.191, $p < 0.001$), 1.006 (95% CI: 1.004–1.008, $p < 0.001$), respectively. Pleural traction, nodular type, nodular shape, age, longest diameter of solid components, solid components of mediastinal window, lobulation sign, spiculation sign and air bronchial sign were not independent risk factors for IA ($p > 0.05$) (Table 3).

TABLE 3 Binary logistic regression analysis of AAH/AIS/MIA group and IA group (not included in intraoperative frozen section)

Item	OR	95% CI	*p*-value
Longest diameter	4.426	2.391–8.191	<0.001
Maximum CT value of ROI	1.006	1.004–1.008	<0.001

Abbreviations: AAH, atypical adenomatoid hyperplasia; AIS, adenocarcinoma in situ; CT, computed tomography; IA, invasive adenocarcinoma; MIA, minimally invasive adenocarcinoma; ROI, region of interest.

TABLE 4 Binary logistic regression analysis of AAH/AIS/MIA group and IA group (included in intraoperative frozen section)

Item	OR	95% CI	*p*-value
Longest diameter	4.450	2.183–9.071	<0.001
Maximum CT value of ROI	1.004	1.001–1.006	0.002
Intraoperative frozen section	45.502	12.617–164.097	<0.001

Abbreviations: AAH, atypical adenomatoid hyperplasia; AIS, adenocarcinoma in situ; CT, computed tomography; IA, invasive adenocarcinoma; MIA, minimally invasive adenocarcinoma; ROI, region of interest.

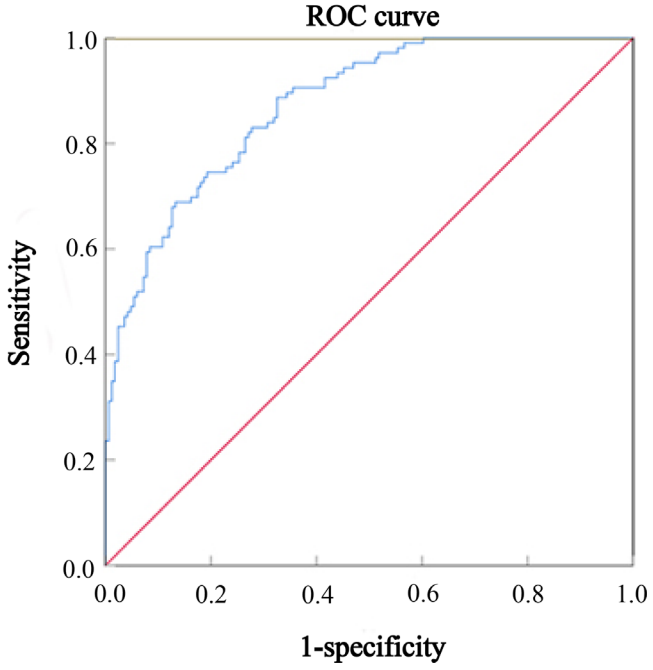

FIGURE 1 The receiver operating characteristic (ROC) curves for the mathematical prediction model (not included in the intraoperative frozen section). The area under the curve (AUC) value using the prediction model was 0.873

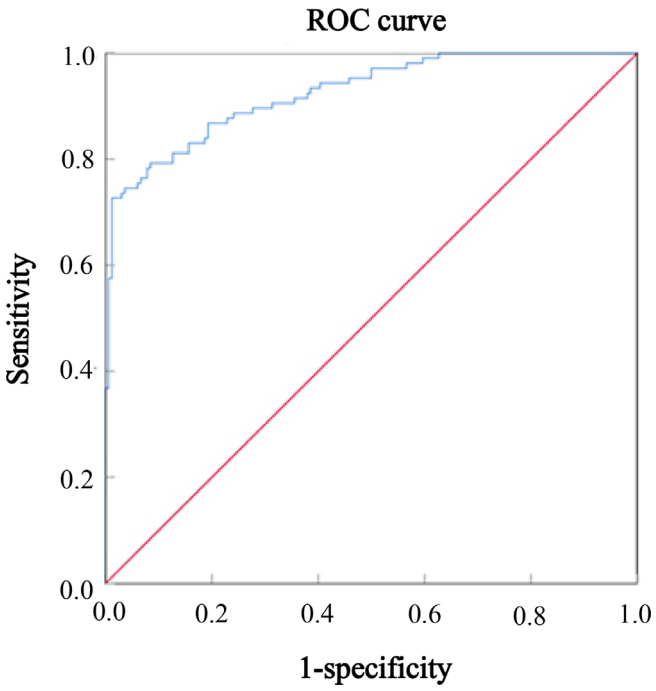

FIGURE 2 The receiver operating characteristic (ROC) curves for the mathematical prediction model (included in the intraoperative frozen section). The area under the curve (AUC) value using the prediction model was 0.925

According to the results of logistic regression analysis, a mathematical prediction model of invasiveness of GGNs was established, and the ROC curve was drawn. The area under the curve (AUC) value was calculated to be 0.873 (95% CI: 0.833–0.913 $p < 0.001$), the sensitivity was 69.8%, the specificity was 82.5%, the positive predictive value was 71.8%, and the negative predictive value was 81.1% (Figure 1).

The other group included FS. The longest diameter, maximum CT value, pleural traction, nodular type, nodular shape, age, longest diameter of solid component, solid component of mediastinal window, lobulation sign, spiculation sign, air bronchus sign and FS were included in the logistic regression analysis. The results showed that the longest diameter, maximum CT value and FS were independent risk factors for IA, and the risk ratios were 4.450 (95% CI: 2.183–9.071, $p < 0.001$), 1.004 (95% CI: 1.001–1.006, $p = 0.002$), 45.502 (95% CI: 12.617–164.097, $p < 0.001$), respectively. Pleural traction, nodular type, nodular shape, age, longest diameter of solid components, solid components of mediastinal window, lobulation sign, spiculation sign and air bronchus sign were not independent risk factors for IA ($p > 0.05$) (Table 4). According to the logistic regression analysis results, a mathematical model for predicting the invasiveness of GGNs was established, and the probability of IA $P = e^X/(1 + e^X)$ was established. $X = -2.881 + (1.493 \times \text{longest diameter of nodules}) + (0.004 \times \text{maximum CT value}) + (3.818 \times \text{FS})$. Where e is the natural logarithm, FS: IA = 1, AAH/AIS/MIA = 0. Based on the modeling data, the ROC curve was drawn, and the AUC value was calculated to be 0.925 (95% CI: 0.893–0.957, $p < 0.001$), the sensitivity was 75.5%, the specificity was 94.0%, the positive predictive value was 88.9%, and the negative predictive value was 85.7% (Figure 2).

Taking the FS as a single predictive factor to establish a prediction model, the ROC curve was drawn, and the AUC value was calculated to be 0.807 (95% CI: 0.747–0.867 $p < 0.001$), the sensitivity was 63.2%, the specificity was

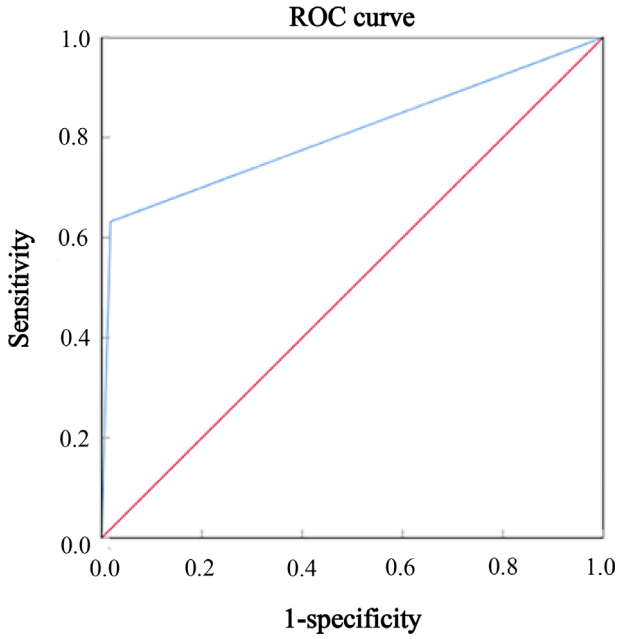

FIGURE 3 The receiver operating characteristic (ROC) curves for the mathematical prediction model (single factor of intraoperative frozen section). The area under the curve (AUC) value using the prediction model was 0.807

98.2%, the positive predictive value was 95.7%, and the negative predictive value was 80.7% (Figure 3).

DISCUSSION

With an increase in the incidence of GGNs in clinical practice, it is very important to diagnose the nature of GGNs. GGNs are not a specific radiological feature. On CT images, GGNs may represent alveolar changes, interstitial changes, pulmonary infection, pulmonary edema or interstitial diseases. However, there is no doubt that "GGN-type" lung adenocarcinoma must be our focus. During GGN surgery, the scope of resection is often determined according to the results of FS, and the accuracy of FS becomes very important. Since the latest revised classification of lung adenocarcinoma was put forward by IASLC/ATS/ERS in 2011, FS in our hospital have been divided into AAH, AIS, MIA and IA. Previous studies have reported no difference in recurrence-free survival (RFS) and overall survival (OS) of AAH, AIS and MIA.[10–12] They are classified as AAH/AIS/MIA group in this study.

In this study, the accuracy of FS diagnosis of IA was 80.7%. Compared with previous studies, this result is not satisfactory. The main reason for the low accuracy was the underestimation of IA. Liu et al.[13] retrospectively studied the clinical data of 803 patients and found that the total coincidence rate between FS and final pathology was 84.4%. When AAH, AIS and MIA were classified as low-risk groups, the total coincidence rate between FS and final pathology reached 95.9%. The main consideration for the low accuracy of FS in judging the invasiveness of GGNs in this study is that (i) a total of 804 patients were included in the study by Liu et al. and only 272 patients were included in our study. The small number of cases included may be the reason for the low diagnostic accuracy of FS. (ii) Liu et al. studied benign nodules in AAH, AIS, MIA and IA. This study did not include cases of benign nodules diagnosed by paraffin-embedded tissue section pathology. (iii) Liu et al. studied solid nodules, pGGNs and m GGNs. All cases included in this study were pGGNs and mGGNs (excluding solid nodules). The above studies are all in agreement that FS is an effective method to guide the resection strategy of GGNs, but its accuracy still needs to be improved. The common causes of FS include large tumor size, tumor close to visceral pleura, interstitial inflammation or fibrosis and no obvious atypia.[14]

In this study, we observed the important CT signs of GGNs. Using univariate analysis, we found that there were significant differences in the longest diameter, maximum CT value, pleural traction, nodular type, nodular morphology, age, longest diameter of solid components, solid components of mediastinal window, lobulation sign, spiculation sign, air bronchus sign and FS in the AAH/AIS/MIA and IA groups. CT signs with statistical differences were analyzed by binary logistic regression analysis, and it was found that the longest diameter and maximum CT value of nodules were independent risk factors of IA. According to the results of the analysis, a mathematical prediction model of CT signs was established (not included in FS). The accuracy of diagnosis of IA was 87.3%, which was significantly higher than that of FS. Yin et al. retrospectively analyzed the CT signs of 200 patients with pGGNs.[15] The results of statistical analysis showed that mean diameter and shape were independent risk factors for lung pGGN pathology as IA. The AUC value of the mathematical prediction model based on independent risk factors was 0.839. The accuracy of the mathematical prediction model of CT signs obtained in this study was higher than that of Yin et al. in the diagnosis of IA. The main reasons were that (i) we had a larger sample size, (ii) our observation of CT signs was more comprehensive, and (iii) the cases we included were pGGN and mGGN, not just pGGN. The results of this study show that the accuracy of the mathematical prediction model of CT signs (not included in FS) in the diagnosis of IA was higher than that of FS.

Previous studies have focused on the accuracy of CT signs or FS in the diagnosis of GGN invasiveness, and this study compared the CT signs with FS; the results are therefore not ideal. We combined CT signs and FS, and carried out binary logistic regression analysis. According to the results of the analysis, a mathematical prediction model (including FS) was established, and the diagnostic accuracy of IA was as high as 92.5%. Compared with the mathematical prediction model of FS and CT signs (not included in FS), the diagnostic accuracy of the mathematical prediction model (including FS) was significantly improved.

In conclusion, there are a variety of models for predicting the invasiveness of lung GGNs. However, the existing prediction models and data analysis methods still

have limitations. Through this study, we found that the accuracy of observing CT signs to predict whether GGNs were IA was higher than that of FS. Combined with CT signs and FS to predict whether GGNs are IA, the diagnostic accuracy is significantly improved. At present, our research has some limitations. First, we have observed few kinds of CT signs. Increasing the frontier of CT signs may further improve the results of the mathematical prediction model. Second, the sample size of this study was small, and further prospective, multicenter studies on a large number of cases are needed to verify the current predictive model.

CONFLICT OF INTEREST

All authors disclose no conflict of interest and no funding for this study.

ORCID

Jizheng Tang https://orcid.org/0000-0002-8195-0766

REFERENCES

1. Jemal A, Bray F, Center MM, Ferlay J, Ward E, Forman D. Global cancer statistics. CA Cancer J Clin. 2011;61:69–90.
2. Chen W, Zheng R, Baade PD, Zhang S, Zeng H, Bray F, et al. Cancer statistics in China, 2015. CA Cancer J Clin. 2016;66:115–32.
3. Aberle DR, Adams AM, Berg CD, et al. Reduced lung-cancer mortality with low-dose computed tomographic screening. N Engl J Med. 2011;365:395–409.
4. Suzuki K, Kusumoto M, Watanabe S, Tsuchiya R, Asamura H. Radiologic classification of small adenocarcinoma of the lung: radiologic-pathologic correlation and its prognostic impact. Ann Thorac Surg. 2006;81:413–9.
5. Baldwin DR, Callister ME, Graham R, Gleeson F. Members of the Guideline Development Group. Pulmonary nodules again? The 2015 British Thoracic Society guidelines on the investigation and management of pulmonary nodules. Clin Radiol. 2016;71:18–22.
6. Cai J, Xu D, Liu S, Cham MD. The added value of computer-aided detection of small pulmonary nodules and missed lung cancers. J Thorac Imaging. 2018;33:390–5.
7. Travis WD, Brambilla E, Noguchi M, Nicholson AG, Geisinger KR, Yatabe Y. International association for the study of lung cancer/american thoracic society/european respiratory society international multidisciplinary classification of lung adenocarcinoma. J Thorac Oncol. 2011;6:244–85.
8. Qiu ZX, Cheng Y, Liu D, Wang WY, Wu X, Wu WL, et al. Clinical, pathological, and radiological characteristics of solitary ground-glass opacity lung nodules on high-resolution computed tomography. Ther Clin Risk Manag. 2016;12:1445–53.
9. Van Schil PE, Asamura H, Rusch VW, et al. Surgical implications of the new IASLC/ATS/ERS adenocarcinoma classification. Eur Respir J. 2012;39:478–86.
10. Yoshizawa A, Motoi N, Riely GJ, Sima CS, Gerald WL, Kris MG, et al. Impact of proposed IASLC/ATS/ERS classification of lung adenocarcinoma: prognostic subgroups and implications for further revision of staging based on analysis of 514 stage I cases. Mod Pathol. 2011;24:653–64.
11. Woo T, Okudela K, Mitsui H, Tajiri M, Yamamoto T, Rino Y, et al. Prognostic value of the IASLC/ATS/ERS classification of lung adenocarcinoma in stage I disease of Japanese cases. Pathol Int. 2012;62:785–91.
12. Kadota K, Villena-Vargas J, Yoshizawa A, Motoi N, Sima CS, Riely GJ, et al. Prognostic significance of adenocarcinoma in situ, minimally invasive adenocarcinoma, and nonmucinous lepidic predominant invasive adenocarcinoma of the lung in patients with stage I disease. Am J Surg Pathol. 2014;38:448–60.
13. Liu S, Wang R, Zhang Y, Li Y, Cheng C, Pan Y, et al. Precise diagnosis of intraoperative frozen section is an effective method to guide resection strategy for peripheral small-sized lung adenocarcinoma. J Clin Oncol. 2016;34:307–13.
14. Chen D, Dai C, Kadeer X, Mao R, Chen Y, Chen C. New horizons in surgical treatment of ground-glass nodules of the lung: experience and controversies. Ther Clin Risk Manag. 2018;14:203–11.
15. Yin K, Wu JL, Qiu TC. Establishment of a model for the diagnosis of invasive adenocarcinoma of the lung with high-resolution CT signs. Chin J Med Imaging. 2019;27:824–8.

How to cite this article: Tang J, Cui Y, Li B, Xue X, Tian F. Mathematical prediction model of computed tomography signs is superior to intraoperative frozen section in the diagnosis of ground-glass nodular invasive adenocarcinoma of the lung. Thorac Cancer. 2021;12:2382–7. https://doi.org/10.1111/1759-7714.14082